

# Coexpression of Genetically Engineered Cyt b5-CYP3A4 Fusion Protein with POR in Sf9 Insect Cells and Functional Characterization of the Expressed Products *in vitro*

Zhangming Xie<sup>1</sup>, Shabbir Ahmed<sup>1</sup>, Wenhui Liu<sup>1</sup>, Sisi Kong<sup>2</sup>, Yingchun Xu<sup>1</sup>, Ting Liu<sup>3\*</sup>, and Shuqing Chen<sup>1\*</sup>

<sup>1</sup>Department of Pharmacology, Toxicology and Biochemical Pharmaceutics, College of Pharmaceutical Sciences, Zhejiang University, Hangzhou 310058, China

<sup>2</sup>Department of Drug Metabolism and Pharmaceutical Analysis, College of Pharmaceutical Sciences, Zhejiang University, Hangzhou 310058, China

<sup>3</sup>Guizhou Provincial Key Laboratory of Pharmaceutics, School of Pharmacy, Guizhou Medical University, Guiyang 550025, China

## Abstract

Human cytochrome P450 3A4 (CYP3A4) is the most abundant phase I drug-metabolizing enzyme in the liver, and approximately 50% of drugs on the market are metabolized by CYP3A4. Therefore, many *in vitro* studies relied on recombinant CYP3A4 as screening tool to evaluate potential drug-drug interactions (DDIs) *in vivo*. However, limited information regarding recombinant CYP3A4 with high catalytic activity is available. So, the present study aimed to obtain recombinant CYP3A4 with high catalytic activity and to characterize its functions *in vitro*. To enhance the catalytic activities of heterologously expressed CYP3A4, the enzyme was fused to cytochrome b5 (b5) tail-to-head, and the fused enzyme was inserted together with NADPH-P450 reductase (POR) into a single plasmid to achieve a simultaneous expression in sf9 cells. Here, substrate binding affinities, enzymatic activities and applications in *in vitro* DDIs of the fused enzyme were investigated. The dissociation constant  $K_d$  of POR-cyt b5CYP3A4 was  $8.3 \pm 0.87 \mu\text{mol/L}$ , the  $Cl_{int}$  ( $Cl_{int} = V_{max}/K_m$ ) was  $8.57 \text{ mL/min/g protein}$  for POR-cyt b5CYP3A4 in the metabolism of testosterone and  $150.3 \text{ mL/min/g protein}$  for midazolam. In addition, the inhibitory constant  $K_i$  of ketoconazole on testosterone metabolism was  $0.013 \pm 0.0038 \mu\text{mol/L}$ . The present results suggested significantly increased substrate binding affinity and enzymatic activity for the fused enzyme. Thus, the construct could be helpful for studying drug metabolisms and DDIs investigation associated with CYP3A4 *in vitro*. In addition, simultaneous expression of the fused enzyme and POR could provide more reproducible results based on a more stable molar ratio of CYP3A4/POR/b5.

**Keywords:** CYP3A4; Fusion protein; Sf9 insect cells; Heterologous expression; Drug metabolism; Drug-Drug interactions

**Abbreviations:** CYP3A4: Cytochrome P450 3A4; POR: Cytochrome P450 oxidoreductase; cyt b5: Cytochrome b5; DDI: Drug-drug interaction;  $Cl_{in}$ : Intrinsic clearance

## Introduction

Members of heme containing cytochrome P450 (CYP) superfamily of enzymes are known to govern the biotransformation of structurally diverse molecules including drugs, chemical carcinogens, steroids and fatty acids [1,2]. Among the CYPs, CYP1A2, 2C9, 2C19, 2D6 and 3A4/3A5 are the most important members and known to involve in the metabolisms of ~80% of marketed drugs and CYP3A4 catalyzes more than 50% [3]. Due to its multi-substrate spectrum and most abundantly expressed CYP isoform in human liver and small intestine, CYP3A4 is a main reason for raising problems of drug-drug interactions (DDIs) [4,5].

DDIs are major risks related to adverse drug reactions (ADRs), especially in older adults and patients on multiple medications [6]. Several clinically related DDIs have resulted in serious toxicities and led to the withdrawals of many drugs from the market [7-9]. Therefore, various *in vitro* studies have been carried out to evaluate the inhibition potential of new drug candidates toward CYP-mediated metabolisms in order to minimize the incidences of clinically relevant DDIs [10,11].

Therefore, many *in vitro* studies relied on recombinant CYP3A4 as screening tool to evaluate potential drug-drug interactions (DDIs) *in vivo*. For this purpose, catalytically active recombinant human CYP3A4 isoform has been successfully expressed in *E. coli* [12], yeast [13], mammalian cells [14,15] and insect cells [16]. Meanwhile, different techniques have also been employed to enhance the enzymatic activity of recombinant CYP3A4, like co-expression and protein fusion [17-19]. However, In these studies CYP3A4, POR and cyt b5

were constructed in separate vectors, resulted in differential proteins expression levels and results reproducibility. So far, no investigation has been made to construct CYP3A4, OR and cyt b5 in one vector and their co-expression.

To address this need, in the current study we have successfully constructed CYP3A4, POR and cyt b5 into pFastBac Dual plasmid and coexpressed them in Sf9 insect cells (Figure S1). The expressed product has been utilized to evaluate the *in vitro* metabolic activities and DDI studies related to CYP3A4.

Various binding regions in CYP3A4 active site have been reported and several DDI studies also carried out based on multiple probe substrates like midazolam, felodipine/nifedipine, and testosterone [20]. Thus, two structurally unrelated probe substrates [21] of CYP3A4, testosterone and midazolam, were selected to study the enzymatic activities of the fused CYP3A4 and evaluated its applications in the DDIs study *in vitro*.

**\*Corresponding authors:** Ting Liu, Guizhou Provincial Key Laboratory of Pharmaceutics, School of Pharmacy, Guizhou Medical University, Guiyang 550025, China, Tel: (86) 851-86908468; E-mail: [t-liu@163.com](mailto:t-liu@163.com)

Shuqing Chen, Department of Pharmacology, Toxicology and Biochemical Pharmaceutics, College of Pharmaceutical Sciences, Zhejiang University, Hangzhou 310058, China, Tel: (86) 571-8820-8411; E-mail: [chenshuqing@zju.edu.cn](mailto:chenshuqing@zju.edu.cn)

**Received:** May 09, 2016; **Accepted:** May 28, 2016; **Published:** June 03, 2016

**Citation:** Xie Z, Ahmed S, Liu W, Kong S, Xu Y, et al. (2016) Coexpression of Genetically Engineered Cyt b5-CYP3A4 Fusion Protein with POR in Sf9 Insect Cells and Functional Characterization of the Expressed Products *in vitro*. J App Pharm 8: 223. doi: [10.21065/1920-4159.1000223](https://doi.org/10.21065/1920-4159.1000223)

**Copyright** © 2016 Xie Z, et al. This is an open-access article distributed under the terms of the Creative Commons Attribution License, which permits unrestricted use, distribution, and reproduction in any medium, provided the original author and

## Materials and Methods

### Materials

Polymerase chain reaction (PCR) primers were synthesized by Sangon Biotech (Shanghai, China). PCR enzymes, Restriction endonuclease, DNA molecular marker, and T4 ligase were obtained from Takara (Tokyo, Japan). Cellfectin reagent, pFastBac Dual vector, DH10Bac-competent cells, Grace's medium and fetal bovine serum were purchased from Invitrogen (Calsbad, CA). *Spodoptera frugiperda* Sf9 insect cells were obtained from Yangshengtang Company (Hainan, China). The pFastBac1-3A4, POR and *cyt b5* were constructed in our lab previously. The primary anti-histidine antibody and Peroxidase-conjugated goat anti-mouse secondary antibody were purchased from Abmart (Shanghai, China) and Jackson ImmunoResearch Laboratories, Inc (Pennsylvania, USA) respectively. Testosterone and 6 $\beta$ -hydroxytestosterone (chemical purity >99.0%) were purchased from Aladdin (Shanghai, China). Midazolam, 1'-hydroxymidazolam and ketoconazole (chemical purity >99.0%) were obtained from National Institutes for Food and Drug Control (Beijing, China). Isocitric dehydrogenase and DL-isocitric acid trisodium were purchase from Sigma-Aldrich (St. Louis, MO). NADPH and NADP<sup>+</sup> were purchased from Roche (Switzerland). Ammonium acetate, MgCl<sub>2</sub>, Tris-HCl, methanol and other chemicals and solvents were analytical grade and obtained from Sinopharm Chemical Reagent Co. (Beijing, China). Chromatographic grade acetonitrile and methanol were purchased from Tedia, Co. (Fairfield, OH, USA). EZ-ECL Kit was purchased from Biological Industries (Israel). Construction of pFastBac Dual-POR-*cyt b5*CYP3A4

Plasmids encoding POR, CYP3A4 and *cyt b5* have been previously constructed in our lab [22,23] used as templates. *POR* was amplified by PCR with oligonucleotides 5'-TCGCTAGCGCCAACGTTTCAT-3' and 5'-TGGTACTGCATGCCTCGAGCT-3' as primers. Followed by digestion with *Nhe*I and *Sph*I, *POR* was ligated to pFastBac Dual plasmid to get pFastBac Dual-POR. *CYP3A4 Not I-Xba*I fragment was amplified by PCR using oligonucleotides 5'-TCTAGATGTGCATGGCTCGAG-3' and 5'-CGGAATTCAAAGGCCTACGTC-3' as primers, and ligated to pFastBac Dual-POR to get pFastBac Dual-POR-CYP3A4. Whereas *cyt b5* was amplified using 5'-GCGTGCACATGGCAGAGCAGT-3' and 5'-TTGCGGCCGCGGGAACCACCACCACCTGCCTCTGCCATGT-3' primers. The underlined sequence served as linker for *cyt b5* gene to be fused with *CYP3A4* gene. The *cyt b5* was digested with *Nhe*I and *Sal*I and ligated to pFastBac Dual-POR-CYP3A4 to get fusion enzyme expression plasmid: pFastBac Dual-POR-*cyt b5*CYP3A4.

### Coexpression of *cyt b5*-CYP3A4 fusion protein with POR

The Bac-to-Bac baculovirus expression system was used to coexpress *cyt b5*-CYP3A4 fusion protein with POR enzyme. The pFastBac Dual-POR-*cyt b5*CYP3A4 plasmid was transformed into competent DH10Bac cells to obtain Bacmid- POR-*cyt b5*CYP3A4. Further, Sf9 cells were transfected with bacmid-POR-*cyt b5*CYP3A4 to get recombinant baculovirus stock. Blank bacmid and recombinant bacmid with blank pFastBac Dual plasmid were used as negative control. All stocks were successively amplified to final titer of 1.0 $\times$ 10<sup>8</sup> pfu/mL.

Shake flask method was used for Sf9 insect cell culture to enhance protein expression level. The conditions were optimized as Sf9 cells were infected with recombinant baculovirus particles, hemin stock solution (2 mg/mL, prepared by dissolving hemin in 50% ethanol and 0.1 mol/L NaOH) was added to culture medium for a final concentration of 2  $\mu$ g/mL. After 72 h incubation infected Sf9 cells were harvested, washed with ice-cold phosphate balanced solution (PBS, pH7.4) and re-suspended

in lysis buffer (1 mmol/L EDTA, 100 mmol/L K<sub>3</sub>PO<sub>4</sub>, 20% glycerol, and 0.1 mmol/L PMSF, pH7.4). The microsomes were prepared by differential centrifugation (19,000 $\times$ g for 15 min and 100,000 $\times$ g for 55 min) after sonication. The final precipitates were resuspended in 100 mmol/L potassium phosphate buffer (pH 7.4) with 20% glycerol [24]. CYP3A4+POR and CYP3A4+POR+*cyt b5* microsomes were also prepared as described and stored at -80°C until further use.

### Immunoblot analysis

Both *cyt b5*-CYP3A4 fusion protein and POR were tagged with histidine (6 $\times$ His), therefore anti-histidine antibody and peroxidase-conjugated goat anti-mouse antibody were served as primary and secondary antibody. The specific method was described previously [22] and was used after minor modification. The microsomes were loaded in SDS-PAGE with 5 $\times$  loading buffer followed by electrophoresis, proteins were transferred from SDS-PAGE to PVDF film at 100 V for 1 h. The PVDF film with proteins were blocked with 5% skim milk in TBST for 2 h at room temperature. The membrane was incubated overnight at 4°C with anti-histidine antibody. The membrane was washed three times with TBST, and incubated with peroxidase-conjugated goat anti-mouse secondary antibody. After three-time washing, the bands were detected with EZ-ECL Kit.

### Determination of P450 and *cyt b5* content and POR activity assay

Sf9 cells were harvested by shake-flask method and washed twice with PBS. Cell pellets were lysed by sonication in the presence of protease inhibitors and the total protein contents were determined by BCA protein assay kit. The microsomal P450 and *cyt b5* concentration were determined by reduced CO-difference spectra assay according to Omura and Sato and nature protocols. The microsome sample was divided into two 1 mL cuvettes and spectrophotometric baseline was recorded between 400 and 500 nm. In one cuvette CO gas was slowly bubbled and 1 mg Na<sub>2</sub>S<sub>2</sub>O<sub>4</sub> was dissolved to each cuvette. The spectrum was recorded between 400 and 500 nm until the peak near 450 nm stopped increasing. The *cyt b5* contents were determined same as above except CO bubbling [25,26].

POR activity was determined by measuring the NADPH-cytochrome *c* reducing activity. The sample was mixed with 80  $\mu$ L of 0.5 mmol/L horse heart cytochrome *c* solution. Spectrophotometer was adjusted at 550 nm in kinetic mode. By adding NADPH solution A550 was measured as the reaction started till A550 plot versus time was no longer linear [26].

### Substrate binding of the expressed microsomes

Substrate binding of CYP3A4+POR, CYP3A4+POR+*cyt b5* and POR-*cyt b5*CYP3A4 microsomes were measured as Hayashi K et al., mentioned [19].

### Testosterone 6 $\beta$ -hydroxylation and Midazolam 1'-hydroxylation

The kinetic parameters for testosterone 6 $\beta$ -hydroxylation and midazolam 1'-hydroxylation were measured as chen et al., mentioned [23].

### Inhibitory effect of ketoconazole on testosterone metabolism

The incubation method and sample preparations were same as above. The concentrations of ketoconazole and testosterone were ranged from 0 to 1.0  $\mu$ mol/L and 10-100  $\mu$ mol/L, respectively. Metabolites were assayed directly by using HPLC as described earlier. Each reaction was conducted in triplicate in three independent experiments.

### Testosterone-midazolam interaction

The effect of midazolam on testosterone 6 $\beta$ -hydroxylation was conducted with 10, 25, 50 and 200  $\mu$ mol/L testosterone and various concentrations of midazolam. Conversely, the effect of testosterone on midazolam 1'-hydroxylation was conducted with 5, 10, 25, 100  $\mu$ mol/L midazolam and different concentrations of testosterone. All the other procedures were same as described earlier. Each reaction was conducted in triplicate in three independent experiments.

## Results

### Immunoblot analysis

To confirm the coexpression of cyt b5-CYP3A4 fusion protein with POR, POR microsomes were used as positive control, and blank bacmid proteins served as negative control. Immunoblot analysis clearly detected protein band at ~78 KDa for POR and for cyt b5-CYP3A4 fusion protein at ~74 KDa (Figure S2) in our coexpressed microsomes.

### Determination of P450 and Cyt B5 content and Por activity assay

The contents of CYP3A4 and cyt b5 in microsomes were determined by P450 and cyt b5 spectral assays. The microsomal protein contents of CYP3A4 and cyt b5 were detected 296.7  $\pm$  11.2 pmol/mL and 326.7  $\pm$  14.8 pmol/mg, respectively. Whereas, the NADPH-cytochrome c reduction activity of POR was found 17.3  $\pm$  0.84 nmol of cytochrome c reduced per min per mg of microsomal protein. While the POR activity towards blank bacmid contents was 1.13  $\pm$  0.08 nmol of cytochrome c reduced per min per mg of microsomal protein.

### Substrate binding of the expressed microsomes

A typical type I spectra was observed by adding testosterone contents to CYP3A4+POR, CYP3A4+POR+cyt b5 and POR-cyt b5CYP3A4 microsomal fractions, indicating the conversion of microsomal heme iron from low to high spin state. The dissociation constant Kd and testosterone concentration were calculated from double-reciprocal plots of  $\Delta$ A390-420 (Figure 1). The CYP3A4 Kd values in CYP3A4+POR+cyt b5 and POR-cyt b5CYP3A4 microsomes were found similar but less than half of the CYP3A4+POR microsomes (Table 1). These results indicated that substrate binding affinity has been modified by cyt b5 but the fusion of cyt b5 to CYP3A4 kept the substrate binding capabilities of CYP3A4.

Substrate-induced differential spectra of CYP3A4+POR, CYP3A4+POR+cyt b5 and POR-cyt b5CYP3A4 microsomes were measured at 22°C and 20, 50, 100 and 200  $\mu$ mol/L testosterone concentrations respectively.

### Testosterone 6 $\beta$ -hydroxylation and Midazolam 1'-hydroxylation

To further validate our co-expressed fused enzymes with POR, apparent  $V_{max}$  and Km values were calculated using nonlinear regression analysis of Michaelis-Menten model (GraphPad Prism 5, Vision 5.01, GraphPad Software Inc.). The apparent  $V_{max}$  and Km for 6 $\beta$ -hydroxytestosterone formation were calculated 22.3  $\pm$  0.31 pmol product/(min $\times$ pmol P450) and 67.0  $\pm$  3.61  $\mu$ mol/L, respectively (Figures 2A and 2B). The  $Cl_{int}$  ( $Cl_{int}=V_{max}/K_m$ ) was found 0.333  $\mu$ L/min/pmol P450. An increased catalytic activity of co-expressed fusion cyt b5-CYP3A4 and POR microsomes for testosterone was observed when compared with previously tri-expressed human CYP3A4, POR and cyt b5 microsomes (Table 2) [24]. While, more than 10% higher C.V values of CYP3A4+POR+cyt b5 than that of POR-cyt b5CYP3A4 has been proven *in vitro*, drug metabolic studies are more replicable using co-expression technique in one vector.

A total 100  $\mu$ L of incubation mixture containing CYP enzyme (2 pmol/L), 100 mmol/L Tris-HCl (pH 7.4), 15 mmol/L MgCl<sub>2</sub> and NADPH generating system (1 unit/mL isocitrate dehydrogenase and 5 mmol/L isocitrate) was used to determine the metabolic against testosterone. In preincubated (37°C for 5 min) samples concentrations were used in the range of 10 to 300  $\mu$ mol/L of testosterone.

The reaction was initiated by adding NADPH/NADP<sup>+</sup> at a final concentration of 1 mmol/L and terminated with double volumes of ice-cold acetonitrile. The mixture, after vortex, was centrifuged at 16,100 $\times$ g for 20 min. 20  $\mu$ L supernatant was assayed by HPLC (Agilent Technologies 1200 system, Santa Clara, CA) with a Dikma Technologies's Diamonsil C18 column (5  $\mu$ m, 200 $\times$ 4.6 mm). The chromatographic separation of 6 $\beta$ -hydroxytestosterone was obtained at 28°C with a flow rate of 1.0 mL/min with an isocratic mobile phase consisting of 45% acetonitrile and detected at 244 nm with VWD detector. Kinetic parameters were determined from three independent experiments in triplicate. In addition, the coefficient of variation (CV) of Kinetic parameters for the testosterone metabolism was calculated to evaluate the reproducibility of the fusion-enzyme-catalyzed metabolisms.

Whereas for 1'-hydroxymidazolam the apparent  $V_{max}$  and Km were found 29.8  $\pm$  1.32 pmol product/(min $\times$ pmol P450) and 5.12  $\pm$  0.667  $\mu$ mol/L, respectively (Figures 3A and 3B) with 5.82  $\mu$ L/min/pmol P450  $Cl_{int}$  ( $Cl_{int}=V_{max}/K_m$ ). Increased  $V_{max}$  (Table 3) has confirmed higher intrinsic clearance of our co-expressed microsomes than previously tri-expressed microsomes [24].

Microsomes	$K_d$ ( $\mu$ M)
CYP3A4 + POR	18.2 $\pm$ 5.9
CYP3A4 + POR + cyt b <sub>5</sub>	8.5 $\pm$ 1.85 <sup>*</sup>
POR-cyt b <sub>5</sub> CYP3A4	8.3 $\pm$ 0.87 <sup>*</sup>

Each value represents the means  $\pm$  SD of three separate experiments.  
<sup>\*</sup>Compared with "CYP3A4 + POR",  $P < 0.05$ .

**Table 1:** Binding affinity of testosterone for CYP3A4+POR, CYP3A4+POR+cyt b<sub>5</sub> and POR-cyt b<sub>5</sub>CYP3A4 microsomes.

microsomes	$K_m$		$V_{max}$		$Cl_{int}=V_{max}/K_m$ (ml/min/g protein)
	( $\mu$ M)	C.V%	( $\mu$ mol/min/g protein)	C.V%	
POR-cyt b <sub>5</sub> CYP3A4	67.0 $\pm$ 3.61 <sup>*</sup>	5.39	0.574 $\pm$ 0.008	1.39	8.57
CYP3A4+POR+cyt b <sub>5</sub> CYP3A4+POR+cyt b <sub>5</sub>	118.6 $\pm$ 13.4	11.3	0.426 $\pm$ 0.120	28.2	3.59

<sup>\*</sup>Compared with "CYP3A4 + POR+cyt b<sub>5</sub>",  $P < 0.05$ .

**Table 2:** Comparison of kinetic parameters for 6 $\beta$ -hydroxytestosterone formation by POR-cyt b<sub>5</sub>CYP3A4 and CYP3A4+POR+cyt b<sub>5</sub> microsomes.

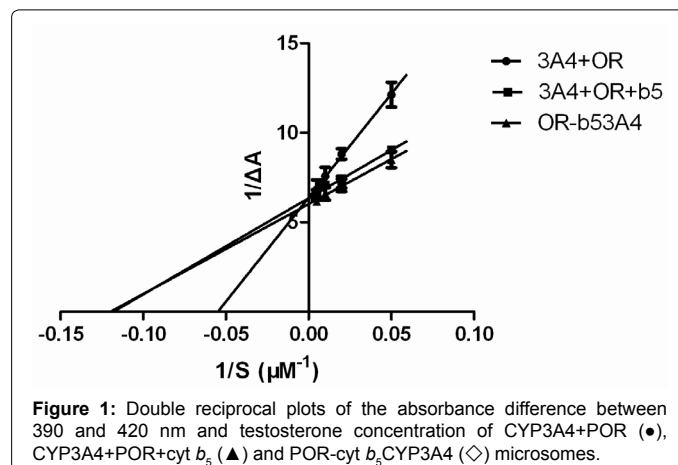


**Figure 1:** Double reciprocal plots of the absorbance difference between 390 and 420 nm and testosterone concentration of CYP3A4+POR (●), CYP3A4+POR+cyt b<sub>5</sub> (▲) and POR-cyt b<sub>5</sub>CYP3A4 (◇) microsomes.

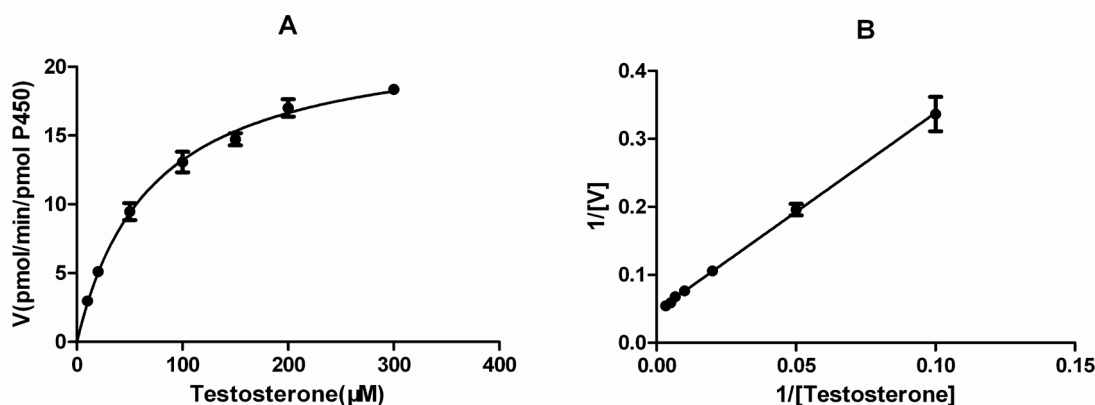


**Figure 2:** Kinetics for testosterone 6β-hydroxylation determined by incubation of testosterone with coexpressed cyt *b*<sub>5</sub>-CYP3A4 fusion protein and POR. **2A.** Michaelis-Menten kinetics graph for 6β-hydroxytestosterone; **2B.** Lineweaver-Burk plot for 6β-hydroxytestosterone. Data are depicted as mean ± S.D. (n=3).

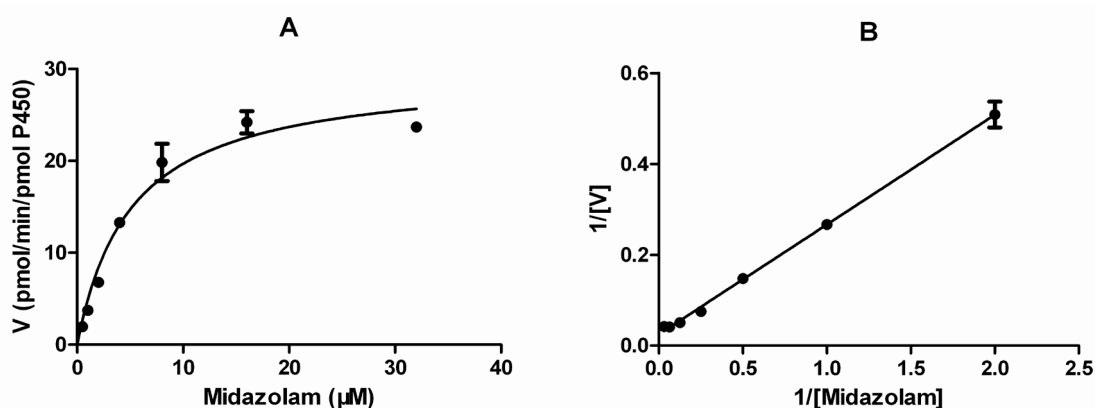


**Figure 3:** Kinetics for midazolam 1'-hydroxylation determined by incubation of midazolam with coexpressed cyt *b*<sub>5</sub>-CYP3A4 fusion protein and POR. **3A.** Michaelis-Menten kinetics graph for 1'-hydroxymidazolam; **3B.** Lineweaver-Burk plot for 1'-hydroxymidazolam. Data are depicted as mean ± S.D. (n=3).

Microsomes	<i>K<sub>m</sub></i> (μM)	<i>V<sub>max</sub></i> (μmol/min/g protein)	<i>Cl<sub>int</sub></i> = <i>V<sub>max</sub></i> / <i>K<sub>m</sub></i> (ml/min/g protein)
POR-cyt <i>b</i> <sub>5</sub> CYP3A4	5.12 ± 0.367	0.77 ± 0.034*	150.3
CYP3A4+POR+cyt <i>b</i> <sub>5</sub>	3.89 ± 0.682	0.49 ± 0.057	126.0

\*Compared with "CYP3A4 + POR+cyt *b*<sub>5</sub>", P<0.05.

**Table 3:** Comparison of kinetic parameters for 1'-hydroxymidazolam formation by POR-cyt *b*<sub>5</sub>CYP3A4 and CYP3A4+POR+cyt *b*<sub>5</sub> microsomes.

A total 100 μL of incubation mixture containing CYP enzyme (2 pmol), 100 mmol/L Tris-HCl (pH 7.4), 15 mmol/L MgCl<sub>2</sub> and NADPH generating system (1 unit/mL isocitrate dehydrogenase and 5 mmol/L isocitrate) was used to determine the metabolic against midazolam. In preincubated (37°C for 5 min) samples concentrations were used in the range of 0.5 to 32 μmol/L of midazolam.

The reaction was initiated by adding NADPH/NADP<sup>+</sup> at a final concentration of 1 mmol/L and terminated with double volumes of ice-cold acetonitrile. The mixture, after vortex, was centrifuged at 16,100×g for 20 min. 50 μL supernatant was assayed by HPLC (Agilent Technologies 1200 system, Santa Clara, CA) with a Dikma Technologies's Diamonsil C18 column (5 μm, 200×4.6 mm). The chromatographic separation of 1'-hydroxymidazolam was detected at

254 nm with a linear gradient elution, at a flow rate of 1.0 mL/min at 30°C. The linear gradient condition for 1'-hydroxymidazolam was 0 min, 20% buffer B; 7 min, 65% buffer B; 13 min, 20% buffer B (buffer A, 10 mmol/L ammonium acetate; buffer B, 10 mmol/L ammonium acetate in 90% acetonitrile and 10% methanol). Kinetic parameters were determined from three independent experiments in triplicate.

### Inhibitory effect of ketoconazole on testosterone metabolism

In present study, to investigate the influences of CYP3A4 inhibitors on testosterone 6β-hydroxylation, a classical CYP3A4 inhibitor, ketoconazole, was used (Figure S3A). Dixon plot was constructed to determine inhibitory constant *K<sub>i</sub>* (Figure S3B). The value of *K<sub>i</sub>* was found (0.013 ± 0.0038 μmol/L) within the FDA reference range (*K<sub>i</sub>*=0.0037~0.18 μmol/L). The results have confirmed the suitability of recombinant microsomes for CYP3A4 inhibition studies *in vitro*.

### Testosterone-midazolam interaction

Testosterone and midazolam are actively metabolized by CYP3A4 [27]. In this study, we have investigated 6β-hydroxytestosterone and 1'-hydroxymidazolam, the major metabolite of testosterone and midazolam, respectively. It is evident from the results that midazolam inhibited testosterone 6β-hydroxylation (Figure 4A) and testosterone inhibited midazolam 1'-hydroxylation (Figure 4B) with prevailing

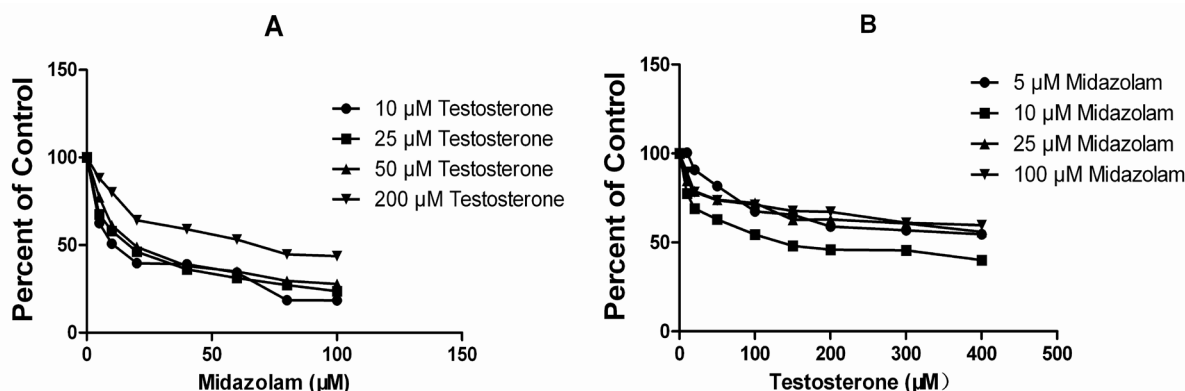


**Figure 4:** Interaction of testosterone and midazolam in the microsomes coexpressed cyt *b5*-CYP3A4 fusion protein and POR. **4A.** Effect of midazolam on testosterone 6 $\beta$ -hydroxylation. The corresponding control activities were 3.0, 5.7, 8.7, and 14.6 pmol product/(min $\times$ pmol P450), respectively; **4B.** effect of testosterone on midazolam 1'-hydroxylation. The corresponding control activities were 12.75, 23.16, 26.19 and 23.19 pmol product/(min $\times$ pmol P450), respectively.

testosterone partial inhibition. These results suggested that the testosterone-CYP3A4-midazolam complex favored the testosterone 6 $\beta$ -hydroxylation pathway rather than the midazolam 1'-hydroxylation pathway.

## Discussion

CYPs are actively involved in the metabolism of numerous exogenous and endogenous compounds including drugs and toxins. Several attempts have been made to express cytochrome P450 proteins in heterologous systems [28,29] and baculovirus expression vector system (BEVS) considered as an efficient system for their expression [30,31]. BEVS has the advantage of posttranscriptional modification events similar to mammalian cells over the available methods. However, the expressions of CYPs and POR using insect cells co-infected with different baculoviruses have been proved difficult to control the expression levels of coexpressed proteins [32]. For heterogenous expression pFastBac-Dual plasmid has provided with two promoters. In present study cyt *b5*, CYP3A4 and POR have been simultaneously expressed in pFastBac-Dual plasmid. This heterogenous expression system led to an easier batch control and replicable results in our drug metabolic studies *in vitro*.

Cytochrome *b5* has been known to support electron transfer from NADPH to CYP3As via the reductase enzyme resulting in enhanced CYP3A4 catalytic properties [33]. In the present study, cyt *b5* and CYP3A4 were fused in tail-to-head between the transmembrane domains, and their activities were not affected by the fusion. The results (Table 1) showed that the cyt *b5* increased substrate binding affinities of CYP3A4 and fusion of cyt *b5* to CYP3A4 kept the substrate binding affinity of CYP3A4. Whereas the direct interaction between cyt *b5* and the CYP3A4 domains modified the tertiary structure of CYP3A4 substrate binding pocket, which resulted in high substrate binding affinities.

To obtain the high expression levels of recombinant proteins, shake-flask culture method was used to facilitate the high insect cell proliferation rate. The Sf9 cell culture conditions were optimized according to Xie et al., [24] with some modifications to get  $3.0 \times 10^7$  cells/mL. Shake-flask culture technique resulted in higher cell densities and increased protein expression levels than T-flask culture method. Therefore, shake-flask culture technique greatly reduced time required for enzymes production and proved economical.

The interactions between CYP3A4 substrates and inhibitors are complex and difficult to predict due to the lack of enzyme

understandings. Korzekwa et al., [34] proposed an appropriate two-site model to interpret *in vitro* studies related to CYP3A4 activities. Whereas, Kenworthy et al., [35] used multisite models for the kinetic analysis of two substrates which were simultaneously metabolized by CYP3A4. For detailed study of *in vitro* DDIs associated with CYP3A4 both models has been used. The prepared microsomes in present study have proved more convenient to obtain and more appropriate for *in vitro* DDIs studies related to CYP3A4 when compared with human liver microsomes. Therefore, the current technique used to develop genetically engineered microsomes could provide the researchers an opportunity of extrapolating DDIs *in vitro* to *in vivo* investigations.

In general, to obtain highly active CYP3A4 microsomes, pFactBac Dual-POR-cyt*b5*CYP3A4 was constructed with stable expression levels and used to study its drug metabolic activities and *in vitro* DDIs. The results proved that the developed technique for fusion of cyt *b5* and CYP3A4 has opened a new window to enhance the substrate binding affinity of CYP3A4, the simultaneous expression of CYP3A4, POR and cyt *b5* microsomes with increased enzymatic activity and stable CYP3A4/cyt *b5*/POR ratios. Therefore, the developed technique to obtain microsomes could be an excellent choice for drug metabolism and *in vitro* DDIs studies related to CYP3A4 and other CYPs.

## Conclusions

This study proved that the substrate binding affinity was increased by fusion of cyt *b5* and CYP3A4. Furthermore, the enzymatic activity of CYP3A4 has been significantly improved by co-expression of the cyt *b5*-CYP3A4 fusion enzyme with POR. The developed technique in present study will be a suitable choice for CYP3A4 or other CYP450s expression and can be a valid reference for future *in vitro* drug metabolism and DDIs investigations.

## Conflict of interest

This work was supported by the National Natural Science Foundation of China [No. 81273578]; National Major Projects for Science and Technology Development of Ministry Science and Technology of China [2012ZX09506001-004]; and Guizhou Science and Technology Department (No. 2013-5002). The authors report no declarations of interest.

## Acknowledgement

Authors' contributions are: Shuqing Chen designed study, Zhangming Xie and Wenhui Liu performed research, Sisi Kong analyzed data, Yingchun Xu contributed important reagents, Zhangming Xie and Ting Liu wrote paper, and Shabbir Ahmed and Ting Liu revised paper. Also, the authors would like to thank Prof. Dr. Su

Zeng (Department of Drug Metabolism and Pharmaceutical Analysis, College of Pharmaceutical Sciences, Zhejiang University) for much constructive discussion during the progress of this research.

## References

1. McDaniel RE, Maximov PY, Jordan VC (2013) Estrogen-mediated mechanisms to control the growth and apoptosis of breast cancer cells: a translational research success story. *Vitam Horm* 93: 1-49.
2. Guengerich FP (2001) Common and uncommon cytochrome P450 reactions related to metabolism and chemical toxicity. *Chem Res Toxicol* 14: 611-650.
3. Orr STM, Ripp SL, Ballard TE, Henderson JL, Scott DO, et al. (2012) Mechanism-Based Inactivation (MBI) of Cytochrome P450 Enzymes: Structure-Activity Relationships and Discovery Strategies to Mitigate Drug-Drug Interaction Risks. *Journal of Medicinal Chemistry* 55: 4896-4933.
4. Rahmioglu N, Le Gall Gnl, Heaton J, Kay KL, Smith NW, et al. (2011) Prediction of Variability in CYP3A4 Induction Using a Combined<sup>1</sup>H NMR Metabonomics and Targeted UPLC-MS Approach. *Journal of Proteome Research* 10: 2807-2816.
5. Hamon V, Horvath D, Gaudin C, Desrivot J, Junges C, et al. (2012) QSAR Modelling of CYP3A4 Inhibition as a Screening Tool in the Context of Drug-Drug Interaction Studies. *Molecular Informatics* 31: 669-677.
6. Huang J, Niu C, Green CD, Yang L, Mei H, et al. (2013) Systematic prediction of pharmacodynamic drug-drug interactions through protein-protein-interaction network. *PLoS Comput Biol* 9: e1002998.
7. Brown HS, Ito K, Galetin A, Houston JB (2005) Prediction of *in vivo* drug-drug interactions from *in vitro* data: impact of incorporating parallel pathways of drug elimination and inhibitor absorption rate constant. *Br J Clin Pharmacol* 60: 508-518.
8. Yao M, Zhu M, Sinz MW, Zhang H, Humphreys WG, et al. (2007) Development and full validation of six inhibition assays for five major cytochrome P450 enzymes in human liver microsomes using an automated 96-well microplate incubation format and LC-MS/MS analysis. *J Pharm Biomed Anal* 44: 211-223.
9. Grime KH, Bird J, Ferguson D, Riley RJ (2009) Mechanism-based inhibition of cytochrome P450 enzymes: an evaluation of early decision making *in vitro* approaches and drug-drug interaction prediction methods. *Eur J Pharm Sci* 36: 175-191.
10. Zientek M, Miller H, Smith D, Dunklee MB, Heinle L, et al. (2008) Development of an *in vitro* drug-drug interaction assay to simultaneously monitor five cytochrome P450 isoforms and performance assessment using drug library compounds. *Journal of Pharmacological and Toxicological Methods* 58: 206-214.
11. Prueksaritanont T, Chu X, Gibson C, Cui D, Yee KL, et al. (2013) Drug-Drug Interaction Studies: Regulatory Guidance and An Industry Perspective. *American Association of Pharmaceutical Scientists* 15: 629-645.
12. Lin HL, Kanaan C, Hollenberg PF (2012) Identification of the residue in human CYP3A4 that is covalently modified by bergamottin and the reactive intermediate that contributes to the grapefruit juice effect. *Drug Metab Dispos* 40: 998-1006.
13. Cheng J, Wan DF, Gu JR, Gong Y, Yang SL, et al. (2006) Establishment of a yeast system that stably expresses human cytochrome P450 reductase: application for the study of drug metabolism of cytochrome P450s *in vitro*. *Protein Expr Purif* 47: 467-476.
14. Gerets HHJ, Tilmant K, Gerin B, Chanteux H, Depelchin BO, et al. (2012) Characterization of primary human hepatocytes, HepG2 cells, and HepaRG cells at the mRNA level and CYP activity in response to inducers and their predictivity for the detection of human hepatotoxins. *Cell Biology and Toxicology* 28: 69-87.
15. Schroer K, Kittelmann M, Lütz S (2010) Recombinant human cytochrome P450 monooxygenases for drug metabolite synthesis. *Biotechnol Bioeng* 106: 699-706.
16. Bakken GV, Rudberg I, Christensen H, Molden E, Refsum H, et al. (2009) Metabolism of quetiapine by CYP3A4 and CYP3A5 in presence or absence of cytochrome B5. *Drug Metab Dispos* 37: 254-258.
17. Parikh A, Gillam EM, Guengerich FP (1997) Drug metabolism by *Escherichia coli* expressing human cytochromes P450. *Nat Biotechnol* 15: 784-788.
18. Voice MW, Zhang Y, Wolf CR, Burchell B, Friedberg T (1999) Effects of human cytochrome b5 on CYP3A4 activity and stability *in vivo*. *Arch Biochem Biophys* 366: 116-124.
19. Hayashi K, Sakaki T, Kominami S, Inouye K, Yabusaki Y (2000) Coexpression of genetically engineered fused enzyme between yeast NADPH-P450 reductase and human cytochrome P450 3A4 and human cytochrome b5 in yeast. *Arch Biochem Biophys* 381: 164-170.
20. Foti RS, Rock DA, Wienkers LC, Wahlstrom JL (2010) Selection of alternative CYP3A4 probe substrates for clinical drug interaction studies using *in vitro* data and *in vivo* simulation. *Drug Metab Dispos* 38: 981-987.
21. Yuan R, Madani S, Wei XX, Reynolds K, Huang SM (2002) Evaluation of cytochrome P450 probe substrates commonly used by the pharmaceutical industry to study *in vitro* drug interactions. *Drug Metab Dispos* 30: 1311-1319.
22. Chen Y, Chen S, Li X, Wang X, Zeng S (2006) Genetic variants of human UGT1A3: functional characterization and frequency distribution in a Chinese Han population. *Drug Metab Dispos* 34: 1462-1467.
23. Chen X, Pan LQ, Naranmandura H, Zeng S, Chen SQ (2012) Influence of various polymorphic variants of cytochrome P450 oxidoreductase (POR) on drug metabolic activity of CYP3A4 and CYP2B6. *PLoS One* 7: e38495.
24. Xie Z, Liu W, Xu Y, Chen S (2013) Optimization of tri-expression of human CYP3A4 with POR and cyt b5 in Sf9 cells. *Journal of Zhejiang University: Medical Sciences (in Chinese)* 42: 38-44.
25. Omura T, Sato R (1964) The carbon monoxide-binding pigment of liver microsomes. I. Evidence for its hemoprotein nature. *J Biol Chem* 239: 2370-2378.
26. Guengerich FP, Martin MV, Sohl CD, Cheng Q (2009) Measurement of cytochrome P450 and NADPH-cytochrome P450 reductase. *Nat Protoc* 4: 1245-1251.
27. Granvil CP, Yu AM, Elizondo G, Akiyama TE, Cheung C, et al. (2003) Expression of the human CYP3A4 gene in the small intestine of transgenic mice: *in vitro* metabolism and pharmacokinetics of midazolam. *Drug Metab Dispos* 31: 548-558.
28. Dong MS, Lee SB, Kim HJ (2013) Co-expression of human cytochrome b5 increases expression of cytochrome P450 3A4 in *Escherichia coli* by stabilizing mRNA. *Protein Expr Purif* 89: 44-50.
29. Mayumi K, Hanioka N, Masuda K, Koeda A, Naito S, et al. (2013) Characterization of marmoset CYP2B6: cDNA cloning, protein expression and enzymatic functions. *Biochem Pharmacol* 85: 1182-1194.
30. Lu H, Ma J, Liu N, Wang S (2010) Effects of heme precursors on CYP1A2 and POR expression in the baculovirus *Spodoptera frugiperda* system. *Journal of Biomedical Research* 24: 242-249.
31. Lu HY, Qiu LL, Yang XJ, Zhang XM, Zhang Z, et al. (2013) Optimization of heme precursors for the expression of human cytochrome P450 2A13 and its co-expression with oxidoreductase in baculovirus/sf9 system. *J Biochem* 153: 555-563.
32. Sokolenko S, George S, Wagner A, Tuladhar A, Andrich JM (2012) Co-expression vs. co-infection using baculovirus expression vectors in insect cell culture: Benefits and drawbacks. *Biotechnology Advances* 30: 766-781.
33. Yamaori S, Yamazaki H, Suzuki A, Yamada A, Tani H, et al. (2003) Effects of cytochrome b5 on drug oxidation activities of human cyto P450 3As: similarity of Cyp3A5 with Cyp3A4 but not Cyp3A7. *Biochemical Pharmacology* 66: 2333-2340.
34. Korzekwa KR, Krishnamachary N, Shou M, Ogai A, Parise RA, et al. (1998) Evaluation of atypical cytochrome P450 kinetics with two-substrate models: evidence that multiple substrates can simultaneously bind to cytochrome P450 active sites. *Biochemistry* 37: 4137-4147.
35. Kenworthy KE, Clarke SE, Andrews J, Houston JB (2001) Multisite kinetic models for CYP3A4: simultaneous activation and inhibition of diazepam and testosterone metabolism. *Drug Metab Dispos* 29: 1644-1651.